

# Experimental research on masonry mechanics and failure under biaxial compression

Ren Xin<sup>\*1</sup>, Jitao Yao<sup>1a</sup> and Yan Zhao<sup>2a</sup>

<sup>1</sup>School of Civil Engineering, Xi'an University of Architecture and Technology, Xi'an 710055, China

<sup>2</sup>School of Civil Engineering, Harbin Institute of Technology, Harbin 150090, China

(Received June 6, 2016, Revised September 7, 2016, Accepted September 9, 2016)

**Abstract.** This study aimed to develop a simple and effective method to facilitate the experimental research on mechanical properties of masonry under biaxial compressive stress. A series of tests on full-scale brick masonry panels under biaxial compression have been performed in limited principal stress ratios oriented at various angles to the bed joints. Failure modes of tested panels were observed and failure features were analyzed to reveal the mechanical behavior of masonry under biaxial compression. Based on the experimental data, the failure curve in terms of two orthotropic principal stresses has been presented and the failure criterion of brick masonry in the form of the tensor polynomial has been established, which indicate that the anisotropy for masonry is closely related to the difference of applied stress as well as the orientation of bed joints. Further, compared with previous failure curves and criteria for masonry, it can be found that the relative strength of mortar and block has a considerable effect on the degree of anisotropy for masonry. The test results demonstrate the validity of the proposed experimental method for the approximation of masonry failure under biaxial compressive stress and provide valuable information used to establish experimentally based methodologies for the improvement of masonry failure criteria.

**Keywords:** biaxial compression; failure criterion; masonry panel; mechanical behavior; experimental study; anisotropy

## 1. Introduction

Masonry, one of the older anisotropic structural materials consisting of block unit and mortar, is a kind of clear directional composite material reflected the disparity of strength in different direction due to the weak mortar joints. Depending upon the orientation of the joints to the stress directions, a number of different failure modes occur under the condition of different stress combinations. Especially under biaxial stress state, it has a mechanical behavior that has not yet been fully investigated. One reason for this lack of knowledge is the highly anisotropic brittle nature of masonry, which makes complicated, difficult and expensive, the realization of reliable experimental tests under conditions of biaxial stress. Due to lack of experimental data, it is almost impossible to establish the strength theory as well as failure criteria of masonry in plane or space. Researchers have long been aware of the significance of joint orientation to the applied stress, however, there have been few attempts to develop a representative biaxial test in different joint orientation. Only in the last several decades have there been some experimental and analytical investigations on the masonry mechanical behavior and failure modes under biaxial stresses.

Page (1981) studied behavior of brick masonry under biaxial compression. He proposed that to define failure under biaxial stress, a three-dimensional surface in terms of the two principal stresses and their orientation to the bed joints is required. A series of biaxial compression tests on half-scale masonry panels, including the largest number of specimens in the history, have been carried out in 5 kinds of bed joints angles under 9 kinds of stress ratios. He observed that masonry mechanical behavior and failure modes were related to the bed joint orientation and the principal stress ratio, simultaneously. However, he didn't put forward the corresponding strength calculation formula.

Plevris and Asteris (2014) utilized the experimental data reported by Page to introduce an anisotropic Neural Networks (NNs) generated 3D failure surface under biaxial stress for masonry for any angle of the joints to the vertical compressive load, which demonstrated the great potential of using NNs for the approximation of masonry failure surface under biaxial compressive stress. The curves generated by the NNs were continuous and smooth, but not convex. This, in mathematical terms, was not easy to be expressed in a functional form.

Naraine and Sinha (1991) studied the behavior of brick masonry under cyclic biaxial compression and obtained that masonry under cyclic biaxial compression can exhibit three distinct stress-strain curves; They proposed a generalized interaction formula for this failure in terms of stress invariant for the range of stress ratios considered. Nevertheless, the biaxial compression specimens involved in the experimental investigation were half-scaled ones probably lead to size effect.

Senthivel and Uzoegbo (2004) experimentally

\*Corresponding author, Associate Professor  
E-mail: [xinren728@hotmail.com](mailto:xinren728@hotmail.com)

<sup>a</sup>Full Professor, E-mail: [yaojitao@163.com](mailto:yaojitao@163.com)

<sup>b</sup>Assistant Professor, E-mail: [zhaoyan\\_hit@163.com](mailto:zhaoyan_hit@163.com)

investigated the failure criteria of unreinforced masonry under biaxial pseudo dynamic loading. This paper described the tests carried out on square grouted unreinforced brick masonry panels with the principal compressive stresses oriented at 0 and 90 degree angles to the bed joints, and a failure surface was obtained in terms of these parameters. The aim of this research was to produce the failure criteria of unreinforced grouted brick masonry panels, for the purpose of a design process. Also, a series of biaxial compression tests on full-scale brick masonry were performed by Badarloo, Tasnimi *et al.* (2009). A failure criterion, with the principal compressive stresses oriented at 0° and 90° angles to the bed joints, was obtained. The results showed that the behavior of grouted unreinforced brick masonry panels was isotropic and the bed joint orientation did not play a significant role in the failure criterion. But, some specimens at other angle of inclination were not included in the tests mentioned above.

Syrmakezis and Asteris (2001) introduced a cubic tensor polynomial to define a general anisotropic failure surface for masonry under biaxial stress and evaluated the strength parameters using the experimental data in Page (1981). The validity of the method was demonstrated by comparing the failure surface with classical experimental results. To overcome the problem requires a plethora of experimental data, Asteris (2013) proposed a simple heuristic new approach, which determined the set of closed surface of the cubic tensor polynomial.

As a conclusion on the literature review, it shows that although the mechanical behavior under biaxial compression has been investigated to some extent experimentally for both clay brick masonry and grouted concrete masonry (Shan and Tang 1988, Liu, Tang *et al.* 2006), and the failure criteria of masonry under biaxial stress state has been studied analytically in the past by some researchers (Ushaksaraei and Pietruszczak 2002, Yang, Li *et al.* 2009, Asteris and Syrmakezis 2009), results of the masonry failure under biaxial stress are not perfect judging from the current situation. What makes it difficult is the development of the mechanical behavior as well as failure criteria of a variety of masonry materials, to a great extent, depend on a large number of experiments under all kinds of plane stress states. However, as is known, compared with structural components, material mechanical performance tests are more complicated and detailed, especially for the

masonry panels under biaxial stress. In the experimental studies mentioned above and other related (Liu, Tang *et al.* 2009, Badarloo, Tasnimi *et al.* 2009), generally, it is necessary to fabricate a set of special loading device to provide bi-directional pressure. It is, actually, an effective way to test the behavior of masonry panel under biaxial stress, and especially suitable for the scale test model with low bearing capacity (Senthivel and Uzoegbo 2004, Naraine and Sinha 1991). But, the test apparatus is relatively complex and higher cost, making it difficult to generalize under the conventional experimental conditions. Moreover, when the bearing capacity of the masonry panel is higher or the size of the block is larger, the test apparatus may not provide enough reaction force and loading space.

This paper reviews researches carried out in the past three decades on the biaxial tests of masonry and describes an experimental investigation into a series of biaxial compression tests of full-scale perforated brick masonry. A comparatively simple test procedure, that can be realized easily in the conventional experimental conditions, is presented to see how the material anisotropy is affected by various factors. Based on the experimental data, failure criterion of brick masonry under biaxial compression is put forward using a second-order tensor polynomial. Further, tests results are compared with previous researches in order to prove the validity of the experimental method and the rationality of the corresponding failure criterion.

## 2. Experimental program

Tests were performed on square brick specimens (masonry panels) with the principal compressive stresses oriented from 0 to 90 degree angles to the bed joints. Ratios of vertical compressive stress  $\sigma_3$  to horizontal compressive stress  $\sigma_1$  of 4.0, 2.0 and 1.0 were used in conjunction with a bed joint angle  $\theta$  with respect to  $\sigma_1$  direction of 22.5°, 45° and 67.5° (Nazar and Sinha 2006). Ratios of  $\sigma_3$  to  $\sigma_1$  of infinity and zero, respectively, corresponded to uniaxial compression normal and parallel to the bed joint. Actually, principal stress ratios of 0.25, 0.5 were obtained from the results using the symmetry of the panels and loading conditions. Here is a brief introduction of the principal stress ratios used in the test, more information will be detailed in Section 2.5.

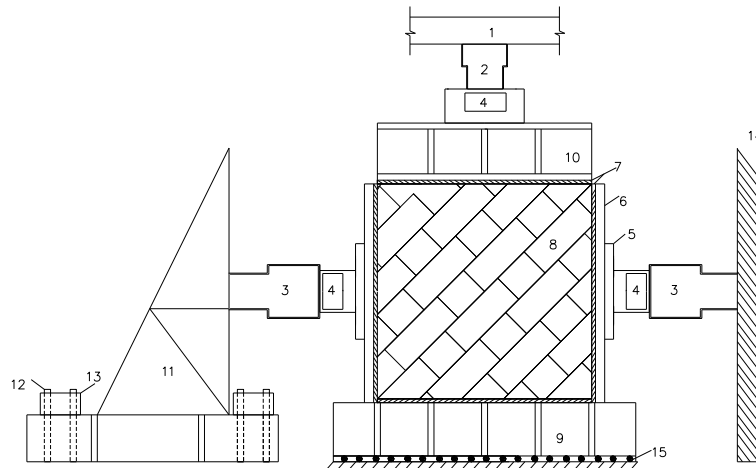


(a) Pre-cut bricks



(b) Specimens with inclinations

Fig. 1 Fabrication of test specimens



(1 Portal rigid frame; 2 Hydraulic jack; 3 Actuator; 4 Load cell; 5 Load transfer plate; 6 Lateral backup plate; 7 PVC plates; 8 Test specimen; 9 Ground beam; 10 Load distribution beam; 11 Reaction frame; 12 Anchor bolt; 13 Compression beam; 14 Reacting-force wall; 15 Steel rollers)

Fig. 2 Testing arrangement

### 2.1 Material properties

The test specimens were constructed with perforated brick of dimensions 240 mm×115 mm×90 mm and void ratio was 22%. Quality control samples were obtained for the bricks and mortar during the construction of all specimens. The mean nominal strength of the bricks based on 9 single units was 9.81 MPa, with a coefficient of variation (Cov) of 0.154. The mean compressive strength of the composite mortar from 12 cubes with a size of 70.7 mm×70.7 mm×70.7 mm was 1.00 MPa and the Cov was 0.233. The composite mortar mix proportion was: 1.0 (cement): 1.5 (lime): 8.0 (sand).

### 2.2 Test specimens

In consideration of the load capacity of the experimental configuration and the scale effect, the square specimen measured 720 mm×720 mm×240 mm, constructed in stretcher bond with full-scale perforated bricks of size 240 mm×115 mm×90 mm and 10 mm thick bed joint mortar. Brickwork was constructed horizontally to ensure a constant joint thickness. Test specimens were made with varying bed joint angles by cutting individual bricks to the shape required before casting (shown schematically in Fig. 1). After cured for 28 days, the hardened specimens were stripped, and left to air dry for a few days before testing.

### 2.3 Test Apparatus

As shown in Fig. 2, the test apparatus was devised to provide vertical pressure via a steel beam of 250 mm depth. The stiffness of the beam was much higher than that of the specimens. A biaxial stress state was induced in the panel by actuator horizontally and by loading vertically with a hydraulic testing machine (jack) with a maximum capacity of 1000 kN. The compression was achieved by setting the load cells with in the reaction frame and reacting-force wall.

The load transfer steel plates were fixed on opposite sides of each specimen so as to guarantee force equality. Several rollers of diameter 10 mm and length 250 mm were placed under the steel ground beam to minimize friction. To minimize the effects of platen constraint on the four sides and thus ensure a more uniform state of stress, the loads were applied to the edges of specimens through some 10 mm thick PVC plate. A constant load ratio was maintained during each test and the load in each direction was monitored by load cells immediately.

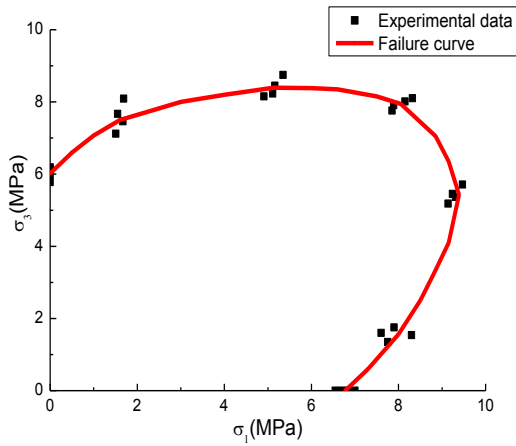
### 2.4 Instrumentation details

The masonry panels were instrumented with LVDTs (linear variable displacement transducers) aligned in two principal directions and diagonal directions over a gauge length of 400 mm on the two free surfaces of the panel to measure the axial, lateral and diagonal displacements. At the same time, 6 electrical resistance strain gauges (ERSG), with lengths of 200 mm, were cemented to the central part of the surfaces in three directions on each side of the panel. The corresponding readings from the two surfaces were averaged to eliminate any bending effects. The load measurement was carried out by installing load cells placed in line with the central axes of the panel and connected to a data-logger system that used to display, monitor and record the load measurements in real time during the test.

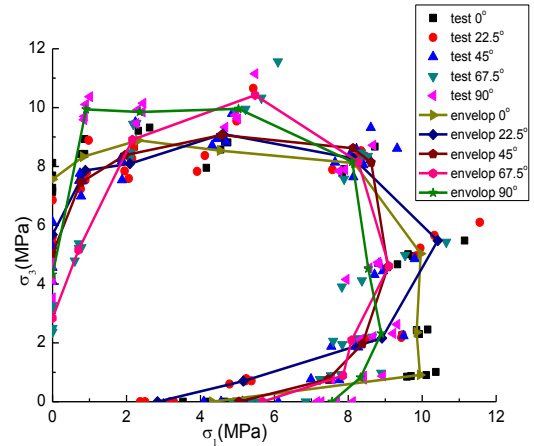
### 2.5 Loading regimes

To avoid eccentricity, preloading within the range of 15% of the ultimate load was repeated two to three times. When the difference between axial deformations in the surfaces was no longer greater than 10%, formal loading began. A monotonic and proportional load was applied, and the ratio of edge loads was kept constant during each test. The following will explain the principle of the determination of load ratio.

In relatively early experimental study (Shan and Tang



(a) Tests results of Naraine and Sinha



(b) Tests results of Page

Fig. 3 Failure of masonry panels under biaxial compression in previous researches



(a) Mortar extruded and cracks appeared



(b) Cracks expanding and deformation out of plane



(c) Failure occurred in the center of the panel



(d) Failure occurred at the edge of the panel



(e) Bricks' face shell flaked off (small number of panels)



(f) Spalling with crushing damage at mid-thickness

Fig. 4 Failure of masonry panels under biaxial compression

1988, Page 1981), load ratios ranged from 0.1 to 10 with many levels (0.1, 0.2, 0.25, 0.5, 0.6, 0.8, 1.0 were often used when the ratio was less than 1.0). In recent years,

many researchers (Liu, Tang *et al.* 2006, Badarloo, Tasnimi *et al.* 2009, Senthivel and Uzoegbo 2004) found that it is not necessary to carry out so much load ratios tests since it

Table 1 Test results for masonry panels

Type of test panels	Orientation of the bed joints ( $\theta$ )	Stress ratio ( $\sigma_1: \sigma_3$ )	Horizontal ultimate stress $\sigma_1^u$ [MPa]	Vertical ultimate stress $\sigma_3^u$ [MPa]	Observed failure modes
UC-A1*			0	-2.440	Splitting
UC-A2	0°	0	0	-2.960	Splitting
UC-A3			0	-2.480	Splitting
BC-B1*		1.0	-3.646	-3.794	Spalling
BC-B2	22.5° (67.5°)	0.5(2.0)*	-2.350	-4.990	Spalling(Off)*
BC-B3		0.25(4.0)	-0.991	-4.200	Spalling(Splitting)*
BC-C1		1.0	-3.129	-2.979	Spalling
BC-C2	45°	0.5	-1.986	-3.900	Splitting(Spalling)*
BC-C3		0.25	-1.080	-4.115	Splitting
BC-D1		1.0	-3.496	-3.457	Spalling
BC-D2	67.5° (22.5°)	0.5(2.0)*	-1.238	-2.464	Splitting(Spalling)
BC-D3		0.25(4.0)	-0.775	-2.999	Spalling(Off)
UC-E1			-1.020	0	Slipping
UC-E2	90°	$\infty$	-0.890	0	Slipping
UC-E3			-0.860	0	Slipping

\*UC-: Uniaxial compressive specimens; BC-: Biaxial compressive specimens; (-): Equivalent panels using the symmetry of the angles and stress ratios; Spalling (Off): Spalling with bricks' face flaked off; Spalling (Splitting): Spalling with local splitting; Splitting (Spalling): Splitting with slight spalling

is close to uniaxial stress state when loading ratios are of great differences. Some key points (i.e., crucial stress ratio), which determine the shape of failure curves or surfaces, are of ratios between 0.2 and 5.0. Naraine and Sinha (1991) utilized the principal stress ratios of 0.2, 0.6, 1.0, 1.67 and 5.0 to obtain a conservative failure curve (shown schematically in Fig. 3(a)). Compared with the tests results of Page (1981) (shown schematically in Fig. 3(b)), the number of the test specimens was down nearly 70 percent.

Based on the previous biaxial compressive strength tests of brick masonry, our current studies utilized some crucial stress ratios of 0.2, 0.5, 1.0, 2.0 and 5.0 in order to approximate the experimental results for brick masonry failure.

### 3. Experimental results

The test masonry panels, including biaxial compression tests were conducted for 22.5°, 45° and 67.5°, and uniaxial compressive specimens of 0 and 90 degree angles to the bed joints, were tested in the experiment, respectively. The compressive strength results of tested masonry panels in various bed joint angles under several crucial stress ratios are shown in Table 1.

#### 3.1 Failure modes

##### 3.1.1 Uniaxial compression

For uniaxial compression normal to the bed joint (i.e., UC-A), failure occurred in a plane (or planes) normal to the plane of the panels, all the cracks passed along the head joints of bricks at alternate courses and through the centre

of the brick at the intervening courses. This failure mode, in fact, was a tension failure tended to occur in weaker bricks. For uniaxial compression parallel to the bed joint (i.e., UC-E), failure initially occurred by splitting in the vertical bed joints due to lateral expansion of the panel and final collapse occurred at higher stress.

It's worth noting that the resulting columns of brick masonry under uniaxial compression were capable of sustaining further load, and the final collapse of the panel occurred at a higher load level. Hence, the compressive strength should be evaluated and the initial cracking strength significantly underestimated the ultimate value.

##### 3.1.2 Biaxial compression

The tests phenomenon showed that the damage process of panels under biaxial compression can be divided into three stages. The first one was called "mortar extruded". The mortar was extruded from bed and head joints gradually accompanied with the compaction of brickwork. Sound of friction and press between mortar and bricks can be heard clearly during the loading process. When the first crack appeared along one mortar joint, this stage came to the end. In the second stage, named "crack propagation", with the increase of pressure load (Ural and Dogangun 2012), cracks expanded slowly along the direction of head and bed joints. However, on account of the presence of the lateral confined principal compressive stress, cracks can't propagate as rapidly as the failure process of uniaxial compression. The splitting failure mode was limited for most specimens of different mortar angles. All the cracks typically passed along the head of bricks at alternate courses and inclined bed joints. At the end of this stage, obvious expansive deformation out of plane occurred on the

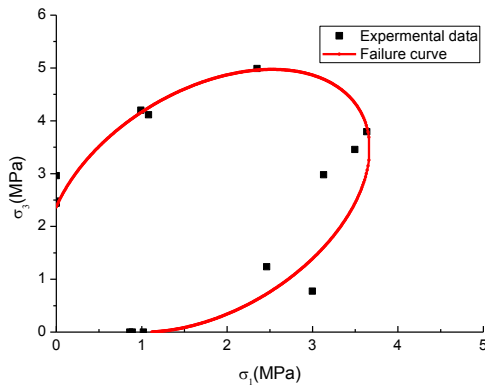


Fig. 5 Failure curve of test results

specimens' surface. Then, the mortar dropped hurriedly from most of the joints and some bricks' face flaked off as ultimate load was reached. Crushing failure, finally, occurred at some portion of the panels by spalling in the plane parallel to the free surface of the specimens at mid-thickness irrespective of the bed joint angles. "Spalling with crushing damage", the so-called the third stage, occurred suddenly in a brittle manner and often began at one of the loaded edges and propagated into the panel. Fig. 4 shows the failure modes of tested masonry panels that were observed for all bed joint angles with various stress ratios considered in this investigation.

### 3.1.3 Analysis of failure modes

Depending on the stress state acting on the panels with varying mortar joint angle, on the one hand, failure can occur in the joints alone, or in some form of combined mechanism involving the joints and bricks simultaneously. On the other hand, panels' damage can appear in-plane or out-of-plane. A series of general failure modes of masonry panels were described by Andraeus (1996), in which the failure modes were divided into three groups, i.e., slipping of mortar joints, cracking of bricks and splitting of mortar joints, and middle plane spalling. The former two groups, according to the differences of stress state and damage position, can be divided in more detail. The above three failure modes, corresponding with Slipping, Splitting, and Spalling, respectively, had taken place in this experiment, shown in Table 1. From the table, it can be seen that not all the test panels damaged in a single mode, in addition, some mixed patterns existed in a small number of panels, especially when the stress ratios were of great differences.

### 3.2 Failure features and regularities

The distinct directional properties of masonry structure were fully verified in present experiments. Under biaxial compression, different failure modes of brick masonry panels were observed depending on the ratio of the principal stress, which showed that the difference of applied stress and the orientation of the bed joints have a considerable effect on the degree of anisotropy for masonry. It behaved strong only when one principal stress predominated and gradually weaker as the stress ratios

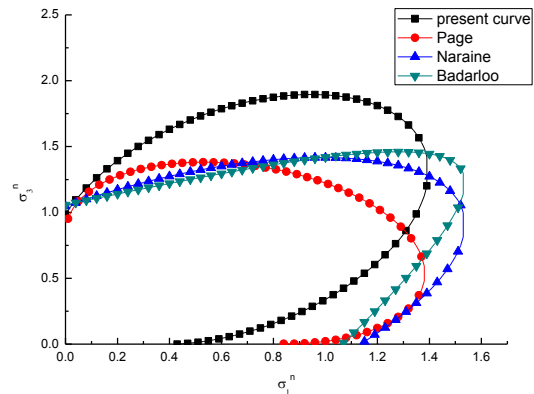


Fig. 6 Experimental failure curves (non-dimensional)

decrease. The greater was the difference between the two principal stress, the easier occur of masonry panels' damaged, especially as the mortar joint angle increased. When the stress ratio was approximately 1.0, the influence of the mortar joint angle was not significant, namely, the masonry seemed to be isotropic in equal biaxial compression.

## 4. Analysis of test results

### 4.1 Failure curves

The failure curves fitted by the ultimate principal stresses from Table 1 are illustrated in Fig. 5. It can be inferred that dominating principal stress increases gradually with the increase of lateral restraining stress. There is an average increase of approximately 50% of the dominating stress at failure as the stress ratio reaches 2.0. That is, the vertical bearing capacity of biaxial compression panels almost doubled compared with the ones under uniaxial compression due to the lateral confining pressure. However, as the levels of restraining stress further increase, there is no pronounced effect of the principal stress ratio on the dominating stress at failure. It is found that the failure features of masonry panels discussed coincide with the failure curves obtained by theoretical fitting.

For the sake of contrastive analysis, the present failure curve and some other ones obtained in previous experiments, have been normalized with respect to uniaxial compressive strength ( $f_{m,cn}$ ), respectively, of which,  $f_{m,cn}$  is the mean strength for uniaxial compression normal to the bed joint (i.e.,  $\theta=0^\circ$ ). A comparison of the failure curves in this investigation with the experimental failure curves reported by Page (1981), Naraine (1991), Badarloo (2009) is shown in Fig. 6. All the failure curves are based on unreinforced brick masonry experiments and plotted in a non-dimensional form. Two orthogonal coordinate axes are represented by  $\sigma_1^n$  and  $\sigma_3^n$ .

Overall, an expected and reasonable comparison is observed. The general shape and trend of the experimental failure curve are close to the investigations mentioned above, but the curve shows a trend towards the strong axis

(i.e., inclined to the  $\sigma_3^n$  axis). It is due to the marked difference of the strength of the two kinds of masonry materials (i.e., relative strength of mortar and block) in this experiment, which result in a relatively obvious difference in the principal strength on the two coordinate axes. In the present study, the ratio of mean orthogonal strengths  $f_{m,cp}/f_{m,cn}$  of the brick masonry panels is approximately 0.4. ( $f_{m,cp}$  is the average uniaxial compressive strength parallel to the bed joint) In contrast, in the test conducted by Page (1981), Naraine (1991), Badarloo (2009), respectively, the ratio of orthogonal strengths was reported to be approximately 0.8, 1.1 and 1.0. Moreover, the size effect of panels has certain effect on the experimental curve. In Page and Naraine's studies, biaxial compression tests were conducted on half-scale brickwork, compared with full-scale masonry panels, with the decrease of specimen size, the anisotropy of masonry becomes weaker. Therefore, compared with other results, the anisotropy of the failure curve proposed in this investigation is more obvious.

## 4.2 Establishment of failure criterion

### 4.2.1 Expression of analytical failure mode

Masonry failure criteria under biaxial stress state have previously been studied by many researchers (Asteris and Syrmakizis 2009, Yang, Li *et al.* 2012). The general failure criterion available for anisotropic materials is the tensor polynomial, which is found to be suitable in defining a failure surface for masonry in the stress space. The form is given in Eq. (1).

$$f(\sigma_k) = F_i \sigma_i + F_{ij} \sigma_i \sigma_j + F_{ijk} \sigma_i \sigma_j \sigma_k + \dots - 1 = 0 \quad (1)$$

where,  $i, j, k=1, 2, \dots, 6$ .  $F_i$ ,  $F_{ij}$  and  $F_{ijk}$  are strength tensors of the second, fourth and sixth rank, respectively. Restricting the analysis to a plane stress state, assuming that a quadratic formation is a reasonably accurate representation of the failure surface and using the notations ( $\sigma_x$ ,  $\sigma_y$ ,  $\tau$ ) instead of ( $\sigma_1$ ,  $\sigma_2$ ,  $\sigma_6$ ), Eq. (1) takes the form

$$\begin{aligned} f(\sigma_x, \sigma_y, \tau) = & F_1 \sigma_x + F_2 \sigma_y + F_{11} \sigma_x^2 \\ & + F_{22} \sigma_y^2 + F_{66} \tau^2 + 2F_{12} \sigma_x \sigma_y - 1 = 0 \end{aligned} \quad (2)$$

The failure criteria of masonry in biaxial compression can be expressed either in terms of the two principal stresses and their orientation to the bed joints, or in terms of a stress state related to the bed joints consisting of a normal stress  $\sigma_n$ , a stress parallel to the bed joints  $\sigma_p$  and a shear stress  $\tau$ . A failure criterion in terms of one of these stress states can be transformed into the alternative failure criterion. However, for biaxial compression, typically for

the failure mode of "middle plane spalling" discussed, a failure criterion in terms of the principal stress system ( $\sigma_1$ ,  $\sigma_3$ ,  $\theta$ ) is more appropriate, as the failure mode for most principal stress ratios is not significantly influenced by the shear stress in the mortar joints. Actually, there is no shear stress during the biaxial compressive tests and then stress  $\tau$  will vanish. The plane stress  $\sigma_x$ ,  $\sigma_y$  will turn into  $\sigma_1$ ,  $\sigma_3$ . Eq. (2) can be further simplified as below

$$F_{11} \sigma_3^2 + F_{22} \sigma_1^2 + F_1 \sigma_3 + F_2 \sigma_1 + 2F_{12} \sigma_1 \sigma_3 = 1 \quad (3)$$

Essentially, Eq. (3) comes from Tsai-Wu failure criterion in plane stress state and has been applied to the failure description of masonry under biaxial stress taking into consideration the anisotropic nature of materials. The corresponding failure curve in plane is a rotated ellipse and the elliptical curve, with the characteristics of non-closed, continuous and convex, is eccentric due to the difference in tensile and compressive strength (Xin and Zhang 2016).

### 4.2.2 Determination of parameters

The determination of the principal strength coefficients  $F_i$ ,  $F_{ii}$  and the interaction strength coefficients  $F_{ij}$  in Eq. (3) are made in two steps. First, concerning factors  $F_i$  and  $F_{ii}$ , these can be readily calculated from the experimentally determined values of uniaxial tensile and compressive strengths (the uniaxial tensile strength tests had been conducted before biaxial tests), this gives

$$\begin{aligned} F_1 = \frac{1}{f_{cp}} - \frac{1}{f_{tp}}, \quad F_2 = \frac{1}{f_{cn}} - \frac{1}{f_{tn}}, \quad F_{11} = \frac{1}{f_{cp} f_{tp}}, \\ F_{22} = \frac{1}{f_{cn} f_{tn}} \end{aligned} \quad (4)$$

where  $f_{cp}$  and  $f_{tp}$  = uniaxial compressive and tensile strength parallel to the bed joint, respectively;  $f_{cn}$  and  $f_{tn}$  = uniaxial compressive and tensile strength normal to the bed joint, respectively. Then, substituting uniaxial test results in present study into Eq. (4), all the principal strength coefficients are obtained in Table 2.

The second step is to determine the interaction strength coefficient  $F_{12}$ , which can be either calculated analytically using the least square method (Syrmakizis and Asteris 2001), or determined from biaxial compression tests. In this paper,  $F_{12}$  is obtained by masonry panels tests under equal biaxial compression, it is acquired

$$2F_{12} = \frac{1 - (F_1 + F_2) f_{ce}}{f_{ce}} - (F_{11} + F_{22}) \quad (5)$$

Table 2 Values of strength coefficients based on experimental results

Calculated by	Undetermined strength coefficients				
	$F_1$	$F_2$	$F_{11}$	$F_{22}$	$F_{12}$
Eq. (4) and Eq. (5)	-6.324	-15.004	8.025	5.856	-3.663
Eq. (4) <sub>n</sub> and Eq. (5) <sub>n</sub> *	-16.606	-39.000	55.428	40.000	-25.261

\*Eq. (4)<sub>n</sub> and Eq. (5)<sub>n</sub>: Calculated by Eq. (4) and Eq. (5) using normalized value

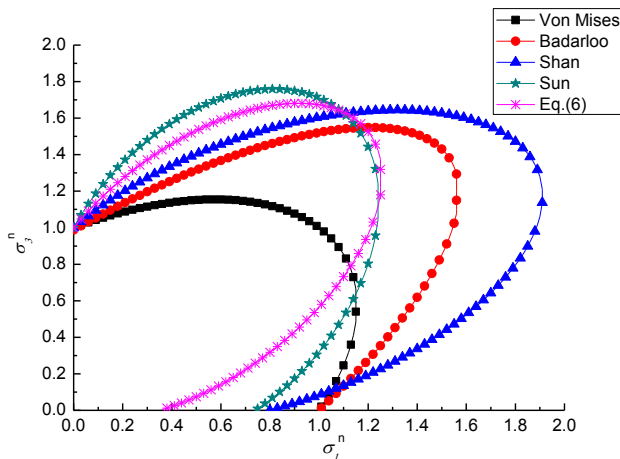


Fig. 7 Comparison of failure criteria

where  $f_{ce}$  = vertical compressive strength under equal biaxial compression. It is substituted the test data in Table 1 into Eq. (5), it can obtain  $F_{12}$  in present study.

#### 4.2.3 Failure criterion

Based on the above calculation results obtained experimentally, it is substituted the Eq. (4) and Eq. (5) into Eq. (3), Eq. (6) can be obtained as below:

$$55.43\sigma_3^{n2} + 40.00\sigma_1^{n2} - 16.61\sigma_3^n - 39.00\sigma_1^n - 50.52\sigma_1^n\sigma_3^n = 1 \quad (6)$$

In order to more efficiently validate the obtained result, it is compared to the main analytical criteria used to define the masonry failure curves and some experimental failure criteria proposed by others based on biaxial compression tests, including: I. Von Mises failure criterion (many modified criterion of masonry have been proposed based upon it); II. Failure criterion of brick masonry under biaxial compressive stress proposed by Shan and Tang (based on the results of a total of 40 full-scale panels under 9 kinds of stress ratios); III. Failure criterion of unreinforced grouted brick masonry based on Badarloo's experiments; IV. Failure criterion proposed by Sun and Tang based on Tsai-Wu tensor theory (derived from the test results of 36 panels of grouted concrete block masonry).

All the failure criteria are expressed in terms of non-dimensional stresses in plane stress state. Fig. 7 shows the comparison between the proposed failure criterion in this investigation and some analytical as well as experimental ones presented above. It can be seen that the proposed failure criterion approximates the experimental results adequately, which demonstrates the fact that, it is reasonable to define masonry failure curves using the tensor polynomial. Due to the difference of the respective two uniaxial compressive strengths, the elliptic curves are not symmetrical about the line  $\sigma_1^n = \sigma_3^n$ .

For the failure criterion proposed in this paper, compared with other failure criteria, the same trend of failure curves is observed from a qualitative perspective. Because of the uncertainty of the test results and the difference of the strength of the tested materials, there is a certain difference in the corresponding failure curves in plane of the failure

criteria given in Fig. 7. In this experiment, the strength of mortar is obviously lower than that of other experiments, leading to the two orthogonal principal stresses differ greatly. Moreover, the greater the two directions of the principal stress difference, the more obvious the characteristic of the material anisotropy.

## 5. Conclusions

With varying principal stress ratios and bed joint orientations, an experimental investigation into a series of tests on full-scale brick masonry panels under biaxial compression have been described in this study. Tests results indicated how the anisotropic strengths are influenced by the orientation of principal stress to bed joint and the stress ratio. Based on the experimental data, a failure criterion has been derived to represent the failure curves of brick masonry under biaxial compressive stress. The following conclusions have been drawn.

- A simple experimental method is presented for masonry under biaxial compression. It provides an approximate way of establishing the failure curve of masonry from a reduced number of biaxial compression tests. The validity of the method is demonstrated by comparing the observed failure modes and derived failure curve with the existing experimental results. The proposed experimental method can be applied in the tests for anisotropic materials under biaxial stress.
- The damage process of masonry panels under biaxial compression can be divided into three stages: mortar extruded, crack propagation and spalling with crushing. The failure modes of masonry are influenced by the ratio of the horizontal to the vertical load and the bed joint orientation. The degree of anisotropy for brick masonry, behaves strong when one principal stress predominates and vanishes in equal applied principal stresses. Also, the relative strength of mortar and block has a considerable effect on the degree of anisotropy.
- The failure curve in terms of two orthotropic principal stresses has been presented, which can be derived from limited biaxial masonry panels of some critical stress ratio. In plane stress state, the curve is an eccentric, non-closed and convex ellipse, and it shows a reasonably good fit with the experimental results. Further, the failure criterion of brick masonry in this study is expressed in the form of the tensor polynomial which reveals the anisotropic features of masonry under biaxial compression. It can be applied for the approximation of the masonry failure under biaxial stress.

## Acknowledgments

The research described in this paper was financially supported by the Natural Science Foundation of China (Grant No. 51508456 and Grant No. 51278401), the Natural Science Foundation of Shaanxi Province (Grant No. 2016JQ5023) and Special Research Fund of Doctor Program for National Higher Education (Grant No.

20106120110005).

## References

- Andreas, U. (1996), "Failure criteria for masonry panels under in-plane loading", *J. Struct. Eng.*, **122**(1), 37-46.
- Asteris, P.G. (2013), "Unified yield surface for the nonlinear analysis of brittle anisotropic materials", *Nonlin. Sci. Lett. A.*, **14**(2), 46-56.
- Asteris, P.G. and Syrmakezis, C.A. (2009), "Non-dimensional masonry failure criterion under biaxial stress state", *11th Masonry Symposium*, Toronto, Canada, June.
- Badarloo, B., Tasnimi, A.A. and Mohammadi, M.S. (2009), "Failure criteria of unreinforced grouted brick masonry based on a biaxial compression test", *Scientia Iranica Transaction A Civil Eng.*, **16**(6), 502-511.
- Dhanasekar, M., Page, A.W. and Kleeman, P.W. (1985), "The failure of brick masonry under biaxial stresses", *Proc. Instn Civ. Engrs, Part 2*, **79**(2), 295-313.
- Liu, L., Tang, D. and Zhai, X. (2006), "Failure criteria for grouted concrete block masonry under biaxial compression", *Adv. Struct. Eng.*, **9**(2), 229-239.
- Liu, L., Tang, D., Zhai, X. and Ma, J. (2009), "Experimental study of grouted concrete block masonry's biaxial compressive strength", *J. HUST*, Urban Science Edition, **26**(3), 18-22.
- Liu, L., Wang, Z., Zhai, C. and Zhai, X. (2010), "Constitutive law of grouted concrete block masonry in plain stress state", *Struct. Eng. Mech.*, **34**(3), 391-394.
- Naraine, K. and Sinha, S. (1991), "Cyclic behavior of brick masonry under biaxial compression", *J. Struct. Eng.*, **117**(5), 1336-1355.
- Nazar, M. and Sinha, S. (2006), "Influence of bed joint orientation on interlocking grouted stabilized mud-flyash brick masonry under cyclic compressive loading", *Struct. Eng. Mech.*, **24**, 585-599.
- Page, A.W. (1981), "The biaxial compressive strength of brick masonry", *Proceedings of the Institution of Civil Engineers Part Research & Theory*, **71**(3), 893-906.
- Plevris, V. and Asteris, P.G. (2014), "Modeling of masonry failure surface under biaxial compressive stress using Neural Networks", *Constr. Build. Mater.*, **55**(55), 447-461.
- Senthivel, R. and Uzoegbo, H.C. (2004), "Failure criterion of unreinforced masonry under biaxial pseudo dynamic loading", *J. South Afri. Inst. Civil Eng.*, **46**(4), 20-24.
- Shan, R. and Tang, D. (1988), "Experimental study of the strength of brick masonry under biaxial compression", *J. Harbin Univ. Civil Eng. Arch.*, **21**(2), 39-46.
- Sun, Z. and Tang, D. (2010), "Failure criterion of grouted concrete block Masonry's biaxial strength", *New Masonry Structural System and Wall Materials-Compilation of Research Results of Reinforced Block Masonry*, July.
- Syrmakezis, C.A. and Asteris, P.G. (2001), "Masonry failure criterion under biaxial stress state", *J. Mater. Civil Eng.*, **13**(1), 58-64.
- Tsai, S.W. and Wu, E.M. (1971), "A general failure criterion for anisotropic materials", *J. Compos. Mater.*, **5**, 58-80.
- Ural, A. and Dogangun, A. (2012), "Crack development depending on bond design for masonry walls under shear", *Struct. Eng. Mech.*, **44**(2), 257-266.
- Ushaksaraei, R. and Pietruszczak, S. (2002), "Failure criterion for structural masonry based on critical plane approach", *J. Eng. Mech.*, **128**(7), 769-778.
- Xin, R. and Zhang, C. (2016), "Experimental research on masonry structure strength under biaxial tensile-compressive stress", *Eng. Mech.*, **33**(10), 183-188.
- Yang, W.J., Li, Y. and Jiang, N. (2012), "The research of masonry failure criterion based on orthogonal anisotropic strength theory", *Adv. Mater. Res.*, **450-451**, 1646-1651.
- Yao, J., Xin, R. and Dong, Z. (2015) "Experimental method of biaxial mechanical properties for masonry structure", China, ZL201210261488.4.

CC